Journal of Radioanalytical and Nuclear Chemistry (2019) 322:2057–2064
https://doi.org/10.1007/s10967-019-06883-1

Measurement of $^{67}Zn(n,p)^{67}Cu$, $^{64}Zn(n,2n)^{63}Zn$, $^{89}Y(n,\gamma)^{90m}Y$ and $^{89}Y(n,2n)^{88}Y$ reaction cross sections at the neutron energy of 14.54 MeV with covariance analysis

Imran Pasha[1] · Rudraswamy Basavanna[1] · Santhi Sheela Yerranguntla[2] · Saraswatula Venkata Suryanarayana[3] · Haladhara Naik[4] · Meghna Karkera[5] · Radha Eswaran[6] · Pandikumar Gurusamy[7] · Sunitha Aladahalli Madegowda[1] · Sachhidananda Hulihalli Basavalingappa[8]

Received: 23 August 2019 / Published online: 29 October 2019

Abstract

The $^{67}Zn(n,p)^{67}Cu$, $^{64}Zn(n,2n)^{63}Zn$, $^{89}Y(n,\gamma)^{90m}Y$ and $^{89}Y(n,2n)^{88}Y$ reaction cross sections relative to the $^{197}Au(n,2n)^{196}Au$ monitor reaction have been determined at the neutron energy of 14.54 ± 0.002 MeV by using the method of activation and off-line γ-ray spectrometry. The neutron energy used was obtained from the $^{3}H(d,n)^{4}He$ reaction. The covariance analysis was performed by taking the uncertainties arising in various attributes and the correlations between those attributes. The analyzed results from the present measurement were compared with the literature data and evaluated data of various libraries like ENDF/B-VIII, JEFF-3.3, JENDL-4.0 and ROSFOND-2010 libraries as well as with the calculated values based on TALYS-1.9 code.

Keywords $^{67}Zn(n,p)^{67}Cu$ · $^{64}Zn(n,2n)^{63}Zn$, $^{89}Y(n,\gamma)^{90m}Y$ and $^{89}Y(n,2n)^{88}Y$ reactions · $^{3}H(d,n)^{4}He$ reaction neutron · γ-Ray spectrometry · Covariance analysis · TALYS-1.9

Introduction

A database of neutron-induced reaction cross sections for high-energy are essential for the construction of D-T fusion reactors, radiation safety, astrophysics, shielding material in accelerator facility, material damage studies, neutron multiplication, nuclear transmutation, accelerator-driven subcritical system, industries and for validation theoretical nuclear models [1, 2]. Among different structural materials, the neutron induced reaction of Zn and Y isotopes are of importance for the above applications. Zinc is a silver-grey, brittle, and lustrous metal, which has five stable isotopes such as ^{64}Zn (64.17%), ^{66}Zn (27.73%), ^{67}Zn (4.04%), ^{68}Zn (18.45%) and ^{70}Zn (0.61%). It is extensively use as structural material in advance fission and fusion reactor technology [2]. Zinc also plays essential role in nuclear forensic and medical applications because the radionuclide ^{63}Zn is a strong positron emitter [3]. On the other hand yttrium is the silvery white metal, lustrous, highly crystalline transition metal and is mono-isotopic element with mass number 89 [4]. Yttrium has applications in X-ray intensifying screens, lasers and is used as an oxide dispersion-strengthened (ODS) ferrite steels, which are expected to be applicant for fuel pin

✉ Haladhara Naik
naikhbarc@yahoo.com

1 Department of Physics, Bangalore University, Bengaluru, Karnataka 560056, India

2 Department of MACS, NITK, Surathkal, Karnataka 575025, India

3 Nuclear Physics Division, Bhabha Atomic Research Center, Mumbai 400085, India

4 Radio Chemistry Division, Bhabha Atomic Research Center, Mumbai 400085, India

5 Department of Statistics, Manipal Academy of Higher Education, Manipal, Karnataka 576104, India

6 RPD, ROMG, IGCAR, Kalpakkam, Tamilnadu 603102, India

7 RSDD, CDG, RDG, IGCAR, Kalpakkam, Tamilnadu 603102, India

8 Visvesvaraya Technological University, Belgaum, Karnataka 590018, India

cladding materials in sodium cooled fast reactor [5]. Thus the accurate cross sections data of ^{89}Y are needed to examine how these materials are affected by neutrons in nuclear reactor [5]. Yttrium is also one of the important fusion reactor material, whose neutron induced reaction cross-section is necessary to determine within the energies of 12–20 MeV [4, 6, 8].

The cross sections data for ^{67}Zn(n,p)^{67}Cu [6–9], ^{64}Zn(n,2n)^{63}Zn [1, 3, 7, 10–13], ^{89}Y(n,γ)^{90m}Y [4, 14–17], ^{89}Y(n,2n)^{88}Y [5, 7, 10, 18–23] reactions are available around the neutron energy of 14 MeV. However, there is comparably huge disagreement [1, 8, 9, 17] and ambiguity in the experimental data, which is most probably due to various nuclear parameters like half-life, γ-ray abundances, monitor cross section and types of detectors used. The neutron induced cross section data for ^{nat}Zn and ^{89}Y is not sufficiently precise for these applications. Thus it is needed to re-measure the neutron induced reaction cross section using more precise nuclear parameters and high resolution γ-ray detection technique [24]. The error free neutron induced reaction cross sections of ^{nat}Zn and ^{89}Y are still not met the requirement and hence need improvement. One more important need is the generation of covariance for the uncertainties of the measured values. Since many of the older experiments do not have data required to generate covariances, the importance of generating covariance data in the context of calculation of uncertainties for nuclear power safety has been stressed by the nuclear data community.

Considering the above facts, measurements of ^{67}Zn(n,p)^{67}Cu, ^{64}Zn(n,2n)^{63}Zn, ^{89}Y(n,γ)^{90m}Y and ^{89}Y(n,2n)^{88}Y reaction cross sections at the neutron energy of 14.54 ± 0.002 MeV have been carried out by using the methods of activation and off-line γ-ray spectrometry. The ^{67}Zn(n,p)^{67}Cu, ^{64}Zn(n,2n)^{63}Zn, ^{89}Y(n,γ)^{90m}Y and ^{89}Y(n,2n)^{88}Y reaction cross sections from the present work were compared with the literature data compiled in EXFOR [25], evaluated data of various libraries and calculated values based on TALYS-1.9 code [26].

Experimental details

The experiment was carried out by using the Purnima neutron generator (PNG) based on the Cockcroft-Walton generator at Bhabha Atomic Research Center (BARC), Mumbai. The deuterium gas was supplied to an RF ion source through which D^+ ions were generated, collected, focused, accelerated and incident on a titanium–tritium (TiT) target. The details of the Purnima neutron generator are given in Ref. [27]. In the current experiment the D^+ ion was accelerated to 180 kV, which was impinged on TiT target.

The ^{nat}Zn, Y and Au metal foils were procured from Alfa Aeaser, USA. The weights of ^{nat}Zn, Y and Au metal foils are 111.0, 25.7, 126.0 mg, respectively. The foils were independently wrapped with 0.011 mm thick Al foil to protect the radioactive contamination from each other during the time of neutron activation. The Zn–Y–Au samples stack was mounted at an angle of zero degrees with respect to the neutron beam direction. The Zn–Y–Au foils stack was irradiated for 2 h with the neutron beam produced from the ^{3}H(d,n)^{4}He reaction. The radioactive samples of Zn–Y–Au along with Al wrapper were mounted on separate Perspex plates and taken for γ-ray spectrometry. The γ-ray counting of the Al wrapped Zn, Y and Au activated foils were counted using a pre-calibrated 185-cc Baltic HPGe detector coupled to a PC-based 4 K multichannel analyzer. A ^{152}Eu standard source used to perform efficiency calibration of the HPGe detector keeping the source at a distance of 1 cm from the detector end cap to decrease summing effect. The resolution of the HPGe detector has a FWHM of 1.8 keV at 1332.5 keV γ-ray photo-peak of ^{60}Co. A detail information of irradiation time, decay time and counting time of the irradiated samples and monitor for the reaction of interest are given in Table 1.

Data analysis

Efficiency calibration of HPGe detector with uncertainty

The ^{152}Eu standard source was used to obtain the efficiency of the HPGe detector. The source activity (A_0) was 5036.89 ± 70.97 Bq as on 1 October 1999. The efficiency of HPGe detector was estimated by the following expression,

$$\varepsilon\left(E_\gamma\right) = \frac{CK_C}{I_\gamma A_0 e^{\ln(2)t/T_{1/2}}} \quad (1)$$

where E_γ is γ-ray energy, $\varepsilon(E_\gamma)$ is efficiency, C is detected γ-ray counts for the counting time of 642 s, $T_{1/2}$ is the half-life (13.517 ± 0.014 years) of ^{152}Eu, t is elapsed time between date of manufacture of source and detector calibration (19.701 years). The half-life and γ-ray branching ratio (I_γ) for each of the eight γ-ray energies of ^{152}Eu were retrieved from NuDat 2.7 [28, 29]. The coincidence summing effect

Table 1 Information related to the irradiation, cooling and counting time

Reaction	Irradiation time (s)	Decay time (s)	Counting time (s)
^{67}Zn(n,p)^{67}Cu	7200	15420	1705
^{64}Zn(n,2n)^{63}Zn	7200	1132	311
^{89}Y(n,γ)^{90m}Y	7200	7551	1677
^{89}Y(n,2n)^{88}Y	7200	7551	1677
^{197}Au(n,2n)^{196}Au	7200	23,193	1006

K_C was determined using EFFTRAN code [30]. The counts and auxiliary data presented in Table 1 are then used in Eq. (1) to obtain efficiency $\varepsilon(E_\gamma)$ at each of the eight identified γ-ray energy and are summarized in column 5 of Table 2.

The corresponding covariance matrix V_ε was obtained by considering the uncertainty information in each of the four attributes C, I_γ, A_o and λ and correlations between them. The methodology for obtaining the covariance matrix is as given in refs. [31, 32].

The known γ-ray energies of ^{152}Eu source is different from the characteristic γ-ray energies of the decay of the reaction products ^{67}Cu, ^{63}Zn,^{90m}Y, ^{88}Y and ^{196}Au. Therefore to determine the efficiency of the detector for the γ-ray of interest from ^{67}Cu, ^{63}Zn,^{90m}Y, ^{88}Y and ^{196}Au nuclides, the following linear parametric function has been considered.

$$In(\varepsilon_i) = \sum_{k=1}^{m} p_k \left(\ln[E_i]\right)^{k-1} 1 \le i \le 8, \tag{2}$$

The best quality of fit was achieved for $n = 4$, with $\frac{\chi^2}{8-4} = 1.58 \approx 1$. The following linear parametric model has been used.

$$ln\varepsilon = -1.93 - 0.92lnE + 0.18(lnE)^2 + 0.12(lnE)^3 \tag{3}$$

Equation (3) was used to estimate the efficiencies corresponding to γ-rays emitted from the decay of the reaction products ^{67}Cu, ^{63}Zn, ^{90m}Y, ^{88}Y and ^{196}Au. Table 3 presents the estimated efficiencies of detector corresponding the reaction products with correlations. The estimated efficiencies presented in Table 2 are required for cross sections calculation. The procedure used in estimating the efficiencies corresponding to the characteristic γ-rays of reaction products with covariance analysis was given in refs. [33, 34].

Neutron energy calculation

Using the parameters of the Purnima neutron generator (PNG) [35], neutron generating head with activation samples is simulated by using GEANT4 code [36]. This code allows the simulation of the interaction of radiation with matter. It is used in applications such as high energy physics, space science, astrophysics, and medical physics, in detector modeling visualization as well as in reverse Monte Carlo simulation [36].

The neutron energy spectrum for a deuteron energy of 180 ± 0.1 keV is simulated using GEANT4, in a convolution with deuteron energy loss and differential cross section. The head geometry and samples are simulated in the geometry class [36]. Deuteron beam diameter, shape, energy and energy spread etc. are also incorporated in the final energy production. Similarly the effect of steel flank, angular coverage of sample are also taken into account. The ENDF/B-VI [37] differential cross section was used for the calculation. A sensitive detector function is defined on the sample to read the energy of neutrons hitting on the sample. The neutron energy data projected into a histogram and normalized with the total number of events. The histogram is further normalized to the total number of counts to get the spectrum. The spectrum obtained from Genat4 is fitted with Gaussian fit

Table 2 Efficiency calibration of HPGe detector using ^{152}Eu standard source with uncertainty

E_γ (keV)	I_γ (%)	C	K_c	$\varepsilon(E_\gamma)$
121.8	28.53 ± 0.16	196497 ± 3438	1.24	7.21E−01 ± 1.67E−2
244.7	7.55 ± 0.04	35202 ± 507	1.35	5.33E−01 ± 1.11E−2
444.0	2.827 ± 0.014	8489 ± 195	1.31	3.33E−01 ± 9.12E−3
688.7	0.856 ± 0.006	1863 ± 130	1.09	2.01E−01 ± 1.43E−2
778.9	12.93 ± 0.08	22363 ± 270	1.23	1.80E−01 ± 3.53E−3
867.4	4.23 ± 0.03	5672 ± 147	1.42	1.62E−01 ± 4.91E−3
964.1	14.51 ± 0.07	22419 ± 316	1.16	1.52E−01 ± 3.12E−3
1408.0	20.87 ± 0.09	23668 ± 427	1.12	1.08E−01 ± 2.51E−3

Table 3 Interpolated efficiencies with uncertainty and correlation matrix

Nuclide	γ-ray Energy (keV)	ε_c	$C_{\varepsilon c}$				
^{67}Cu	184.6	0.6372 ± 0.0125	1				
^{63}Zn	669.6	0.2131 ± 0.0037	0.562	1			
^{90m}Y	202.5	0.6065 ± 0.0121	0.993	0.575	1		
^{88}Y	898.0	0.1599 ± 0.0027	0.515	0.949	0.511	1	
^{196}Au	355.7	0.3958 ± 0.0075	0.861	0.805	0.898	0.681	1

using origin. The neutron energy spread is calculated from the standard deviation of a fitted Gaussian as (FWHM/centroid). The neutron energy is found to be 14.54 ± 0.002 MeV.

^{67}Zn(n,p)^{67}Cu, ^{64}Zn(n,2n)^{63}Zn, ^{89}Y(n,γ)^{90m}Y and ^{89}Y(n,2n)^{88}Y reaction cross-sections with uncertainty calculation

To estimate the ^{67}Zn(n,p)^{67}Cu, ^{64}Zn(n,2n)^{63}Zn, ^{89}Y(n,γ)^{90m}Y and ^{89}Y(n,2n)^{88}Y reaction cross sections for the neutron energy of 14.54 ± 0.002 MeV, the following expression has been used.

$$\sigma_s = \sigma_M \frac{C_S \lambda_S W t_M a_M A_{VS} I_{\gamma M} \varepsilon(E_\gamma)_M \left(1 - e^{-\lambda t_{iM}}\right)\left(e^{-\lambda t_{dM}}\right)\left(1 - e^{-\lambda t_{cM}}\right)}{C_M \lambda_M W t_S a_S A_{VM} I_{\gamma S} \varepsilon(E_\gamma)_S \left(1 - e^{-\lambda t_{iS}}\right)\left(e^{-\lambda t_{dS}}\right)\left(1 - e^{-\lambda t_{cS}}\right)} \prod_k \frac{(C_k)_m}{(C_k)_S} \tag{4}$$

The subscripts S and M appearing in Eq. (4) represent the sample and monitor. $\sigma_s(E_n)$ and $\sigma_M(E_n)$ at the neutron energy E_n represent the reaction cross sections. C_S and C_M are the detected photo-peak counts of the γ-rays corresponding to the reaction products. λ_S and λ_M represent decay constants, Wt_S and Wt_M represent weights. a_S and a_M represent isotopic abundances, A_{VS} and A_{VM} represent average atomic masses, $I_{\gamma S}$ and $I_{\gamma M}$ represent the γ-ray γ-ray branching ratios, $\varepsilon(E_\gamma)_S$ and $\varepsilon(E_\gamma)_M$ represent efficiencies. t_i, t_d and t_C represent irradiation, decay and counting time, $(C_k)_S$ and $(C_k)_M$ represent the correction factors of dead time, where k represent the dead time of the detector and γ-ray self-attenuation factor (Γ_{attn}). The self-attenuation factor (Γ_{attn}) has been estimated, whereas mass attenuation coefficient μ was retrieve from XMuDat ver. 1.0.1 for the irradiated foils using procedure given in refs. [38, 39]. The monitor cross section of ^{197}Au(n,2n)^{196}Au reaction at the neuron energy of 14.54 ± 0.002 MeV was obtained by linear interpolation method, which is 2.1236 ± 0.0205 barns [40].

The basic nuclear spectroscopic data with their uncertainties were retrieved from NuDat 2.7 database [29] and are summarized in Table 4. The terms that are observed with error are σ_M, C_S, C_M, λ_S, λ_M, Wt_S, Wt_M,a_S, A_{VS},A_{VM}, $I_{\gamma S}$, $I_{\gamma M}$,$\varepsilon(E_\gamma)_S$, $\varepsilon(E_\gamma)_M$, $(\Gamma_{attn})_S$ and $(\Gamma_{attn})_M$, whereas other terms such as a_M,t_i, t_d, t_C appearing in Eq. (4) have negligible uncertainties.

The ith and jth entries of covariance matrix $V_{\sigma S}$ [41] corresponding reaction products were estimated as follows.

$$(V_{\sigma S})_{ij} = \sum_{kl} (e_k)_i (s_{kl})_{ij} (e_l)_j, \quad 1 \le i,j \le 3, 1 \le k,l \le 16 \tag{5}$$

where $(s_{kl})_{ij}$ is the correlation between the kth attribute in the ith experiment and lth attribute in the jth experiment and $(e_k)_i = \frac{\partial \sigma_{Si}}{\partial (x_k)_i} \Delta(x_k)_i$, $(e_l)_j = \frac{\partial \sigma_{Sj}}{\partial (x_l)_j} \Delta(x_l)_j$ is partial uncertainties in σ_{Si}, σ_{Sj} due to the kth and lth attributes, respectively. The fractional uncertainties of different parameters in obtaining the ^{67}Zn(n,p)^{67}Cu, ^{64}Zn(n,2n)^{63}Zn, ^{89}Y(n,γ)^{90m}Y and ^{89}Y(n,2n)^{88}Y reactions cross section relative to ^{197}Au(n,2n)^{196}Au monitor reaction are presented in Table 5. The correlations observed between different observations are presented in the sixth column of Table 5. The readers are suggested to refer the Refs. [31, 41, 42] for more details on micro-correlations. The measured results for the ^{67}Zn(n,p)^{67}Cu, ^{64}Zn(n,2n)^{63}Zn, ^{89}Y(n,γ)^{90m}Y and ^{89}Y(n,2n)^{88}Y reaction cross sections at the 14.54 ± 0.002 MeV neutron energy with uncertainties and correlations are summarized in Table 6.

Results and discussion

The ^{67}Zn(n,p)^{67}Cu, ^{64}Zn(n,2n)^{63}Zn, ^{89}Y(n,γ)^{90m}Y and ^{89}Y(n,2n)^{88}Y reaction cross sections have been measured relative to ^{197}Au(n,2n)^{196}Au monitor reaction at the neutron energy range of 14.54 ± 0.002 MeV by using the methods of activation and off-line γ-ray spectrometric technique. The mono-energetic neutron used was obtained from the ^{3}H(d,n)^{4}He reaction. The ^{152}Eu standard source was used to perform efficiency calibration of the HPGe detector. The cross sections of four different reactions were determined using the ratio method. The covariance analysis was performed by taking uncertainties arising in various

Table 4 Nuclear spectroscopic values of nuclide essential for the determination of reaction cross-section ($\sigma_s(E_n)$)

Nuclear reaction	Threshold energy (MeV)	Product nuclide	Half-life	γ-ray energy (keV)	γ-ray branching ratio (%)	Mode of decay (%)
^{67}Zn(n,p)	0.0	^{67}Cu	61.83 ± 0.12 h	184.6	48.7 ± 0.3	β^-(100)
^{64}Zn(n,2n)	12.049	^{63}Zn	38.47 ± 0.05 m	669.6	8.2 ± 0.3	ε (100)
^{89}Y(n,γ)	0.0	^{90m}Y	3.19 ± 0.06 h	202.5	97.3 ± 0.4	IT (100)
^{89}Y(n,2n)	11.61	^{88}Y	106.627 ± 0.021 d	898.0	93.7 ± 0.3	ε (100)
^{197}Au(n,2n)	8.114	^{196}Au	6.1669 ± 0.0006 d	355.7	87 ± 3	ε(93) + β^-(7)

Table 5 Fractional uncertainties (%) with correlations in various attributes of measured reactions

Attributes	^{67}Cu	^{63}Zn	^{90m}Y	^{88}Y	Correlation
σ_M	0.965	0.965	0.965	0.965	Fully correlated
C_S	9.901	2.727	10.60	9.667	Uncorrelated
C_M	0.929	0.929	0.929	0.929	Fully correlated
λ_S	1.121E − 02	9.014 E-02	1.537E − 01	5.554E − 04	Uncorrelated
λ_M	0.654	0.654	0.654	0.654	Fully correlated
Wt_S	2.582E − 02[a]	2.582E − 02[b]	1.123E − 01[c]	1.123E − 01[d]	a and b fully correlated similarly c and d are fully correlated
Wt_M	2.283E − 02	2.283E − 02	2.283E − 02	2.283E − 02	Fully correlated
a_S	3.960[a]	1.525[b]	–	–	a and b fully correlated and c and d are found to be with no error
A_{VS}	1.195E − 05[a]	1.095E − 05[b]	1.912E − 05[c]	1.912E − 05[d]	a and b uncorrelated and c and d are fully correlated
A_{VM}	3.046E − 07	3.046E − 07	3.046E − 07	3.046E − 07	Fully correlated
$I_{\gamma S}$	0.6160	3.658	0.4.111	0.32017	Uncorrelated
$I_{\gamma M}$	0.3448	0.3448	0.3448	0.3448	Fully correlated
$\varepsilon(E_\gamma)_S$	1.966	1.741	1.992	1.674	Uncorrelated
$\varepsilon(E_\gamma)_M$	1.885	1.885	1.885	1.885	Fully correlated
$(\Gamma_{attn})_S$	0.6348	0.2587	0.1189	0.3421	Uncorrelated
$(\Gamma_{attn})_M$	0.6542	0.6542	0.6542	0.6542	Fully correlated

Table 6 The measured reaction cross sections with uncertainty and correlations

Reaction	Cross section (mb)	Correlation			
^{67}Zn(n,p)^{67}Cu	49.95 ± 5.61	1			
^{64}Zn(n,2n)^{63}Zn	176.29 ± 9.76	0.095	1		
^{89}Y(n,γ)^{90m}Y	0.54 ± 0.06	0.047	0.096	1	
^{89}Y(n,2n)^{88}Y	1005.59 ± 101.69	0.054	0.105	0.053	1

attributes and the correlations between those attributes. The ^{67}Zn(n,p)^{67}Cu, ^{64}Zn(n,2n)^{63}Zn, ^{89}Y(n,2n)^{88}Y and ^{89}Y(n,γ)^{90m}Y reaction cross sections as a function of neutron energy were calculated using the TALYS-1.9 code [26].

TALYS code is a software for the calculation of nuclear reaction cross sections based on physics models and parameterizations. It calculates nuclear reaction cross-sections for the targets with mass larger than 12 atomic mass unit and projectiles like photon, neutron, proton, ^{2}H, ^{3}H, ^{3}He and alpha particles in the energy range from 1 keV to 200 MeV. Calculation of nuclear reaction cross-sections includes the direct interaction, pre-equilibrium and compound nucleus contributions. The pre equilibrium contribution can be calculated by two component excitation model. Pre-equilibrium emission takes place after the first stage of the reaction but long before statistical equilibrium of the compound nucleus is attained. For the calculation of reaction cross section, the important parameters are the gamma-ray transmission coefficient and level density parameter. Gamma-ray transmission coefficient is important for the description of the γ-ray emission channel in nuclear reactions. On the other hand, level density parameter is the most important ingredient, which permits to explore the mechanism of nuclear excitations and information about the structure of the excited nuclei. Variation of nuclear level density can be done by using the Generalised superfluid model (GSM) and Back-shifted Fermi gas model (BFM) available in TALYS [26]. In Back-shifted Fermi gas model the energy-dependent level density parameter a is given as

$$a = a(E_x) = \tilde{a}\left[1 + \delta W \frac{1 - e^{-\gamma U}}{U}\right] \tag{6}$$

where U is the excitation energy and γ is the shell damping parameter. δW is the shell correction of nuclear binding energy, which magnitude establishes how a differ from $\tilde{a}$ at low energy. The asymptotic level density parameter $\tilde{a}$ is given as

$$\tilde{a} = \alpha A + \beta A^{2/3} \tag{7}$$

where A is the mass number, and α, β are the global parameters, which determined to give the best average level density.

In the present work, he ^{67}Zn(n,p)^{67}Cu, ^{64}Zn(n,2n)^{63}Zn, ^{89}Y(n,2n)^{88}Y and ^{89}Y(n,γ)^{90m}Y reaction cross sections within the neutron energies of 12–20 MeV were calculated using the default option of the TALYS-1.9 code [26]. The default values of α, β and γ used in the present calculation based on constant temperature model (CTM) are 0.0692, 0.2827 and 0.433, respectively. The ^{67}Zn(n,p)^{67}Cu, ^{64}Zn(n,2n)^{63}Zn and ^{89}Y(n,γ)^{90m}Y and ^{89}Y(n,2n)^{88}Y reaction cross sections at the neutron energy of 14.54 ± 0.002 MeV from the present work and the literature data from the EXFOR [25] compilation within the neutron energies of 12–20 MeV are plotted in Figs. 1, 2, 3, and 4. For comparison, the evaluated data from ENDF/B-VIII.0 [43], JEFF-3.3

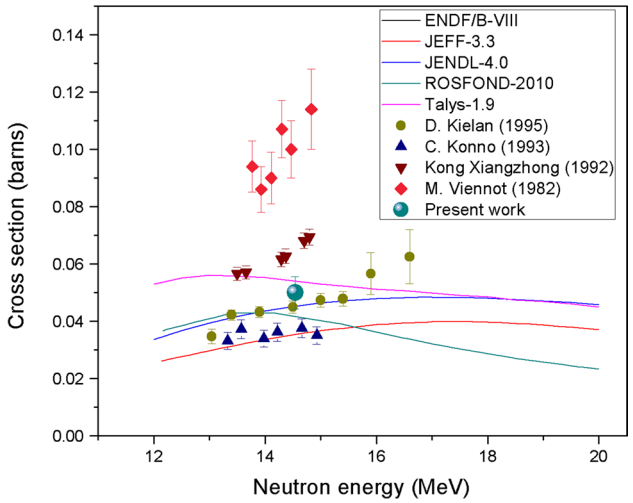

Fig. 1 Plot of $^{67}Zn(n,p)^{67}Cu$ reaction cross section from the present work along with the literature data, evaluated data of ENDF/B-VIII.0, JEFF-3.3, JENDL-4.0 and ROSFOND-2010 libraries as well as with TALYS-1.9 as a function of neutron energy

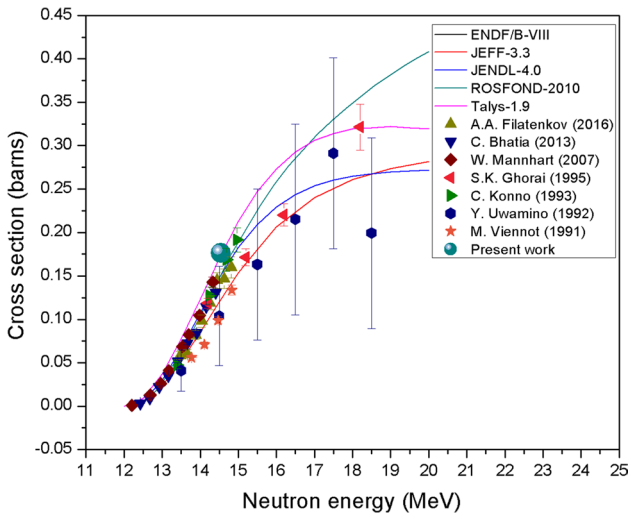

Fig. 2 Plot of $^{64}Zn(n,2n)^{63}Zn$ reaction cross section from the present work along with the literature data, evaluated data of ENDF/B-VIII.0, JEFF-3.3, JENDL-4.0 and ROSFOND-2010 libraries as well as with TALYS-1.9 as a function of neutron energy

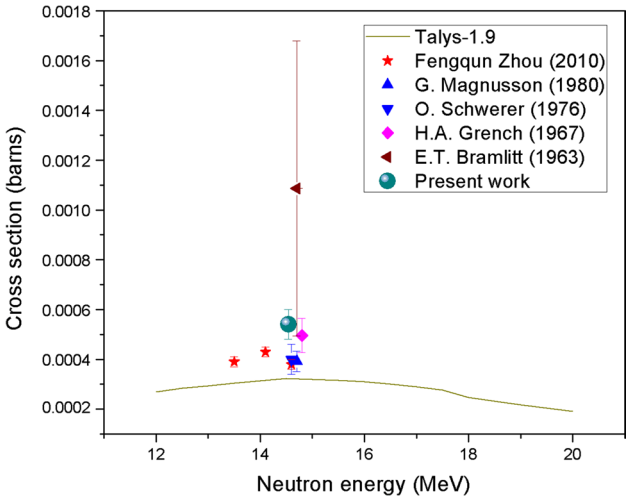

Fig. 3 Plot of $^{89}Y(n,\gamma)^{90m}Y$ reaction cross section from the present work along with the literature data and with the theoretical value from TALYS-1.9 as a function of neutron energy

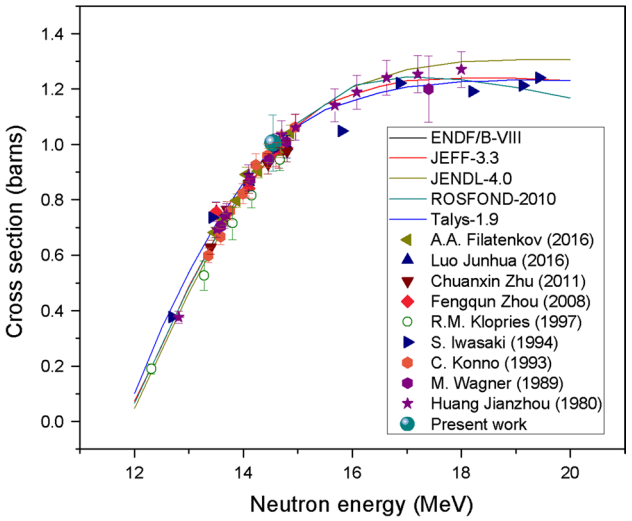

Fig. 4 Plot of $^{89}Y(n,2n)^{88}Y$ reaction cross section from the present work along with the literature data, evaluated data of ENDF/B-VIII.0, JEFF-3.3, JENDL-4.0 and ROSFOND-2010 libraries as well as with TALYS-1.9 as a function of neutron energy

[44], JENDL-4.0 [45] and ROSFOND-2010 [46] libraries as well as calculated values from TALYS-1.9 code [26] within the neutron energies of 12–20 MeV are also plotted in Figs. 1, 2, 3, and 4. Since, the evaluated data for the $^{89}Y(n,\gamma)^{90m}Y$ reaction are not available, only the calculated values from TALYS-1.9 code [26] within the neutron energies of 12–20 MeV are only shown in Fig. 3.

It is can be seen from Fig. 1 that the measured $^{67}Zn(n,p)^{67}Cu$ reaction cross section at the neutron energy of 14.54 ± 0.002 MeV is in good agreement with the value of Kielan et al. [6], which are in between the values of Konno et al. [7] and Xiangzhong et al. [8]. However, the data of Vinnot et al. [9] are significantly higher than the present data and literature data [7, 8]. Figure 1 also shows that the present data and literature data [7, 8] are in agreement with the calculated value from TALYS-1.9 [26] and with the evaluated data of ENDF/B-VIII, JEFF-3.1, JENDL-4.0, ROSFOND-2010 and CENDL-3.1 libraries.

For the $^{64}Zn(n,2n)^{63}Zn$ reaction, Fig. 2 shows that the measured cross section from the present work is slightly higher than the literature data [1, 3, 7, 10–13]. Figure 2

also shows that the present and literature data [1, 3, 7, 10–13] within the neutron energies of 12–20 MeV are in close agreement with the evaluated data of ENDF/B-VIII.0 [43], JEFF-3.3 [44], JENDL-4.0 [45] and ROSFOND-2010 [46] libraries, as well as the calculated values from TALYS-1.9 code [26].

In the case of ^{89}Y(n,γ)^{90m}Y reaction, Fig. 3 shows that the measured cross section from the present work is slightly higher than the literature data [4, 14–16] but significantly lower than the data of Bramlitt et al. [17]. Figure 3 also shows that the ^{89}Y(n,γ)^{90m}Y reaction cross section from the present work and literature data [4, 14–17] within the neutron energies of 12–20 MeV are higher than the calculated values from TALYS-1.9 code [26]

For the ^{89}Y(n,2n)^{88}Y reaction, the measured cross section from the present work at the neutron energy of 14.54 ± 0.002 MeV is in very good agreement with the literature data [5, 7, 10, 18–23]. Figure 4 also shows that the data from the present work and literature [5, 7, 18–23] within the neutron energies of 12–20 MeV are in agreement with the evaluated data of ENDF/B-VIII.0 [43], JEFF-3.3 [44], JENDL-4.0 [45] and ROSFOND-2010 [46] libraries as well as the calculated values from TALYS-1.9 code [26].

Summary

The ^{67}Zn(n,p)^{67}Cu, ^{64}Zn(n,2n)^{63}Zn, ^{89}Y(n,γ)^{90m}Y and ^{89}Y(n,2n)^{88}Y reaction cross sections have been measured relative to the ^{197}Au(n,2n)^{196}Au monitor reaction at incident neutron energy of 14.54 ± 0.002 MeV using the methods of activation and off-line γ-ray spectrometry. A ^{152}Eu standard source was used for the efficiency calibration of HPGe detector. The covariance analysis was performed by taking uncertainties arising in various attributes and the correlations between those attributes. The measured cross sections for the ^{67}Zn(n,p)^{67}Cu, ^{64}Zn(n,2n)^{63}Zn and ^{89}Y(n,2n)^{88}Y reactions have been compared and seen to be in good agreement with the evaluated data of various libraries and the literature data compiled in EXFOR as well as with the calculated values from TALYS-1.9. The measured cross section for the ^{89}Y(n,γ)^{90m}Y reaction has also been compared and seen to be in close agreement with the literature data compiled in EXFOR and calculated value from TALYS-1.9.

Acknowledgement One of the author (BR) would like to thank, Department of Atomic Energy and Board of Research in Nuclear Sciences (DAE-BRNS) through major research project (Sanction No. 36(6)/14/92/2014-BRNS/2727). The authors are grateful to staff of Purnima neutron generator for their excellent operation of accelerator.

References

1. Uwamino Y, Sugita H, Kondo Y, Nakamura T (1992) Measurement of neutron activation cross sections of energy up to 40 MeV using semi-monoenergetic p-Be neutrons. Nucl Sci Eng 111:391–403
2. Bhike M, Saxena A, Roy BJ, Choudhury RK, Kailas S, Ganesan S (2009) Measurement of ^{67}Zn(n,p)^{67}Cu, ^{92}Mo(n,p)^{92m}Nb and ^{98}Mo(n,γ)^{99}Mo reaction cross sections at incident neutron energies of En = 1.6 and 3.7 MeV. Nucl Sci Eng 162(2):175–182
3. Bhatia C, Tornow W (2013) Measurement of ^{64}Zn(n,2n)^{63}Zn reaction cross section between 12.5 and 14.5 MeV. J Phys G: Nucl Part Phys 40:065104
4. Zhou F, Xue X, Kong X, Yuan S, Huang H, Li Y (2010) Measurement of the 89Y(n, γ)90mY cross section in the neutron energy range of 13.5–14.6 MeV. Nucl Instrum Methods Phys Res B 268:1367–1369
5. Luo J, Jiang Li (2016) Activation cross section for reactions induced by d-T neutrons on natural Yttrium. Nucl Sci Eng 184(2):254–262
6. Kielan D, Marcinkowski A (1995) Cross sections for (n, p) reaction on Zinc isotopes in terms of the novel multistep compounds reaction model. Z Phys A 352:137–143
7. Konno C, Ikeda Y, Oishi K, Kawade K, Yamamoto H, Maekawa H (1993) Activation cross section measurements at neutron energy from 13.3 to 14.9 MeV. Report No. JAERI-1329
8. Xiangzhong K, Yongchang Wang, Junqian Y, Jingkang Y, Yongging S (1992) The cross section measurements for 67Zn(n, p)67Cu and 66Zn(n,2n)65Zn reactions. J JLNZ 28:99
9. Viennot M, Ait Haddou A, Chiadli A, Paic G (1982) Excitation functions of (n,p) reactions in the region 13.75 to 15 MeV for Ti, Fe and Ni isotopes. In: Conference on nuclear data for Science and technology, Antwerp, 406
10. Filatenkov AA (2016) Neutron activation cross sections measured at KRI in neutron energy region 13.4–14.9 MeV. INDC (CCP)-0460 Rev, pp 1–290
11. Mannhart W, Schmidt D (2007) Measurement of neutron activation cross sections in the energy range from 8 to 15 MeV. Phys Tech Bundesanst, Neutronenphysik Report No. 53
12. Ghorai SK, Sylva PM, Williams JR, Alford WL (1995) Partial neutron cross sections for ^{64}Zn, ^{66}Zn, ^{67}Zn and ^{68}Zn between 14.2 and 18.2 MeV. Ann Nucl Energy 22:11–22
13. Vennot M, Berrada M, Paic G, Joly S (1991) Cross section measurements of (n, p) and (n, np + pn + d) reactions for titanium, chromium, iron, cobalt, nickel and zinc isotopes around 14 MeV. Nucl Sci Eng 108(3):289–301
14. Magnusson G, Andersson P, Bergqvist I (1980) 14.7 MeV neutron capture cross section measurements with activation technique. Phys Scr 21:21–26
15. Schwerer O, Winkler-Rohatsch M, Warhanek H, WInkler G (1976) Measurement of cross sections for 14 MeV neutrons capture. Nucl Phys A 264:105–114
16. Grench HA, Coop KL, Menlove HO, Vaughn FJ (1967) A study of the spin dependence of the nuclear level density by means of the 89Y(n, γ)90 g, 90mY reactions. Nucl Phys A 94:157–179
17. Bramlitt ET, Fink RW (1963) Rare nuclear reactions induced by 14.7 MeV neutrons. Phys Rev 131(6):2649–2663
18. Zhu C, Chen Y, Mou Y, Zheng P, He T, Wang X, An L, Guo H (2011) Measurement of (n,2n) reaction cross sections at 14 MeV for several nuclei. Nucl Sci Eng 169:188
19. Zhou F, Zhang H et al (2008) Cross section measurements for (n,2n) and (n, α) reactions on Yttrium at neutron energies from 13.5 to 14.6 MeV. Appl Radiat Isot 66:1898–1900

20. Klopries RM, Doczi R, Sudar S, Csikai J, Qaim SM (1997) Excitation functions of some neutron threshold reactions on ^{89}Y in the energy range of 7.8 to 14.7 MeV. Radiochim Acta 79:3–7
21. Iwasaki S, Matsuyama S, Ohkubo T, Fukuda H, Sakuma M, Kitamura M (1994) Measurement of activation cross sections for several elements between 12 and 20 MeV. In: Conference on nuclear data for science and technology, Gatlinburg, vol 1, 305
22. Wagner M, Winkler G, Vonach H, Buczko Cs M, Csikai J (1989) Measurement of the cross sections for the reactions ^{52}Cr(n,2n)^{51}Cr, ^{66}Zn(n,2n)^{65}Zn, ^{89}Y(n,2n)^{88}Y and ^{96}Zr(n,2n)^{95}Zr from 13.5 to 14.8 MeV. Ann Nucl Energy 16:623–635
23. Jianzhou H, Hanlin L, Jizhou L, Peiguo F (1980) Excitation curve measurement for the reaction ^{89}Y(n,2n)^{88}Y. Chin J Nucl Phys 3(2):213
24. Zhang Y, Zhao L, Kong X, Liu R, Jiang L (2012) Cross-sections for (n,2n) and (n, α) reactions on 55Mn isotopes around neutron energy 14 MeV. Radiat Phys Chem 81:1563–1567
25. IAEA-EXFOR Database available at http://www-nds.iaea.org/exfor
26. Koning AJ, Hilaire S, Goriely S (2017) TALYS-1.9, A Nuclear Reaction Program (NRG-1755 ZG Petten, The Netherlands). http://www.talys.eu/download-talys/
27. Sinha A, Roy T, Yogesh K, Ray N, Shukla M, Patel T, Bajpai S, Sarkar PS, Bishnoi S (2015) Experimental subcritical facility driven by D-D/D-T neutron generator at BARC, India. Nucl Instrum Methods Phys Res B 350:66–70
28. Martin MJ (2013) Nuclear data sheets for $A = 152$*. Nucl Data Sheets 114:1497–1847
29. NuDat 2.7 (2016) National Nuclear Data Center, Brookhaven National Laboratory. http://www.nndc.bnl.gov/nudat2
30. Vidmar T (2005) EFFTRAN—a Monto Carlo efficiency transfer code for gamma-ray spectrometry. Nucl Instrum Methods Phys Res A 550:603–608
31. Sheela SY, Naik H, Prasad KM, Ganesan S, Suryanarayana SV (2017) Detailed data sets related to covariance analysis of the measurement of cross section of ^{59}Co(n,γ)^{60}Co reaction relative to the cross section of ^{115}In(n,γ)^{116m} In: Internal Report No. Mu/Stastics/DAE-BRNS/2017. https://doi.org/10.13140/rg.2.2.26729.49764
32. Geraldo LP, Smith DL (1990) Covariance analysis and fitting of germanium gamma-ray detector efficiency calibration data. Nucl Instrum Methods Phys Res A 290:499–508
33. Pasha I, Rudraswamy B, Radha E, Sathiamoorthy V (2018) Efficiency of high-purity germanium detector at characteristic gamma energies of ^{198}Au and ^{58}Co and covariance analysis. Radiat Prot Environ 41:110–114
34. Geraldo LP, Smith DL (1989) least square methods and covariance matrix applied to the relative efficiency calibration of a Ge(Li) detector. Inst de Pesquisas Energeticas e Nuleares 243:1–16
35. Patel T, Sinha A (2013) Development of low energy deuteron accelerator based DC and pulsed neutron generators. BARC newsletter, 146
36. Agostinelli S et al (2003) GEANT4: a simulation toolkit. Nucl Instrum Methods Phys Res A 506:250–303
37. Carlson AD, Poenitz WP, Hale GM, Peelle RW, Doddler DC, Fu CY, Mannhart W (1993) The ENDF/B-VI neutron cross sections measurement standards. NISTIR5177
38. Millsap DW, Landsberger S (2015) Self-attenuation as a function of gamma ray energy in naturally occurring radioactive material in the oil and gas industry. Appl Radiat Isot 97:21–433
39. Nowotny R (1998) XMuDat photon attenuation data on PC. IAEA Report IAEA-NDS 195. http://www-nds.iaea.org/publications/iaea-nds
40. Capote R, Zolotarev KI, Pronyaev VG, Trkov A (2012) Updating and extending the IRDF-2002 dosimetry library. http://www-nds.iaea.org/IRDFF/
41. Yerraguntla SS, Naik H, Karantha MP, Ganesan S, Suryanarayana SV, Badwar S (2017) Measurement of ^{59}Co(n,γ)^{60}Co reaction cross sections at the effective neutron energies of 11.98 and 15.75 MeV. J Radioanal Nucl Chem 314(1):457–465
42. Pasha I, Basavanna R, Yerranguntla SS, Suryanarayana SS, Meghna K, Naik H, Prasad MK, Danu LS, Saroj B, Petel T, Rajeev K (2019) 93Nb(n,2n)92mNb, 93Nb(n, α)90mY and 92Mo(n, p)92mNb reactions at 14.78 MeV and covariance analysis. J Radioanal Nucl Chem 320:561–568
43. Herman M, Trkov A, Capote GR, Nonre GPA, Brown DA, Arcilla R, Danon Y, Plompen A, Mughabghab SF, Jing Q, Zhigang G, Tingjin L, Hanlin L, Xichao R, Leal L, Carlson BV, Kawano T, Sin M, Simakov Stanislav P, Guber K (2018) Evaluation of neutron reactions on iron isotopes for CIELO and EDNF/B-VIII.0. Nucl Data Sheets 148:214–253
44. Koning AJ, Bauge E, Dean CJ, Dupont E, Fisher U, Forrest RA, Jacqmin R, Leeb H, Kellet MA, Mills RW, Nordborg C, Pescarine M, Rungma Y, Rullhusen P (2011) Status of the JEFF nuclear data library. J Korean Phys Soc 59:1057–1062
45. Shibata K, Iwamot O, Nakagawa T, Iwamot N, Ichihara A, Kunieda S, Chiba S, Furutaka K, Otuka N, Ohasawa T, Murata T, Matsunobu H, Zukeran A, Kamada S (2011) JENDL-4.0: a new library for nuclear science and engineering. Nucl Sci Techol 48:1–30
46. Zabrodskaya SV, Ignatyuk AV, Koscheev VN (2007) Nuclear constants. ROSFOND-2010, pp 1–2